

# Load Position and Residual Vibration Control of an Offshore Crane System Based on Input-Output Linearization Theory

Nhat-Binh Le\* · Kwon-Soon Lee\*\* · † Young-Bok Kim

\*Graduate School, Department of Mechanical System Engineering, Pukyong National University

\*\*Department of Electric Engineering, Dong-A University

† Department of Mechanical System Engineering, Pukyong National University

**Abstract** : In the offshore crane system, the requirements on the operating safety are extremely high due to many external factors. Rope extension is one of the factors producing vertical vibration of load. In this study, the load is carried by the motor-winch actuator control and the rope is modeled as a mass-damper-spring system. To control the load position and suppress the vertical vibration of the load, a control system based on input-output linearization method is proposed. By the simulation and experiment results with pilot crane model, the effectiveness of proposed control method is evaluated and verified.

**Key words** : Load Position, Residual Vibration, Rope Dynamics, Input-Output Linearization, Off-Shore Crane System

## 1. Introduction

Nowadays, the demand of offshore crane system shown in Fig 1. is increasing for exploitation and transportation. Comparing with other operations, the operating safety requirements of crane are extremely high to avoid wrong operations, accidental collisions and so on.

In general, offshore crane systems placed on the vessel transfer loads from one place to another. Then, fast and accurate positioning of load with small vibration is the ultimate control objective. But, there are many external factors affecting the normal operating conditions and parameters variation due to change of rope length or load weight. These facts are represented by time-varying functions such that the dynamic modeling and system control design are too difficult and complex [1][14].

A lot of dynamic load positioning systems have been presented based on linear or nonlinear control theories [3][8][9][12], and applied to the real offshore crane systems [4][5][15] for keeping good working performance. For examples, adaptive observer and two external models [10], sliding mode control [2][13][17], non-linear control based on Lyapunov stability theory [7][16] and other interesting approaches can also be found in [6][18][19].

However, in the previous researches, the controller design process is too complex and hard to apply to the real systems. Furthermore, very simple dynamic models without considering of precise dynamic characteristics are used for control system design. And, in these articles, any case of considering rope stiffness or damping constant has not been found. Based on the high safety requirements on crane operating, the vertical load motion should be carefully



Fig 1. An offshore crane installed on the vessel

† 교신저자, 정회원, kpjiwoo@pknu.ac.kr 051)629-6197

\*학생회원, binhln@vaa.edu.vn 051)629-6197

\*\*정회원, kslee@dau.ac.kr

(주) 이 논문은 “A Study on Load Vibration Control in Crane Operating”의 제목으로 “한국항해항만학회 2017년도 추계학술대회”(부산 관광공사 아르피나, 2017.11.02.-03)에 발표되었음.

considered to guarantee the high operability of the crane especially in the vertical direction.

In this paper, dynamic models of crane and rope which is assumed to be extendable are derived. In the crane system, there are many nonlinear terms and time varying parameters. The representative one is rope stiffness which should be carefully treated in modeling and control system design process to occupy better control performance.

For this issue, based on input-output linearization theory, the authors design a controller to obtain good control performances, such as controlling load position accurately and suppressing vertical vibration of load effectively.

Then, the remainder of this paper is structured as follows. In part 2, the authors present the mathematical modeling of the offshore crane system. Especially, the model of the motor-winch, the equivalent mass in vertical motion, the extension of the rope and the load position dynamics in the experimental apparatus are represented for designing the control system. And, input-output linearization theory is applied to design a controller in part 3. In part 4, the comparing results are shown using experiment study. Finally, conclusions are drawn in part 5.

## 2. Modeling

### 2.1 Experiment setup

At first, the authors introduce the experimental setup which is illustrated in Fig. 2. The controlled plant consists of rope, DC motor, pulley, winch and mass.

Especially, in this paper, we consider that the moving range of mass (load) is constrained in the specified value. Because the author design a control system to suppress the vibration and obtain a desirable control performance in the loading and unloading process which are operated in short distance and is final operating(work) process.

In the experimental apparatus, a spring is inserted between the pulley and load on purpose as shown Fig. 3. It is to consider the dynamic characteristic when the rope is long and extended in real condition. There is no doubt about this assumption.

The data acquisition program is utilized in labVIEW language 9.0. National Instrument PCI 6259 card is used to communicate between motor driver, encoder, distance sensor and experimental computer. The specification of the experimental apparatus is depicted in Table 1.

The main object of crane work is moving the load in the

vertical direction as illustrated in Fig. 2 and Fig. 3. And the authors assume that the crane system is fixed on the land site. The winding winch is located at the top of the crane and works as a main actuator to control the load position and suppress the vertical vibration.

Table 1 Specification of experimental setup

Item	Parameter	Value
Motor	Maxon 334067	
	Voltage [V]	24
	Rated current [A]	2
	Rated speed [RPM]	6910
	Rated power [W]	48
	Gear reduction ratio	27.5
Sensor	Keyence UD-300	
	Sensing range [mm]	300~3000
Winch	Radius [m]	0.05
Load	Mass [kg]	2
Load cell	CASKOREA CBA-100L	
	Rated output [mV/V]	3.0±0.3
Transducer amplifier	CASKOREA LCT-II	
	Voltage output transmitter [V]	0~10

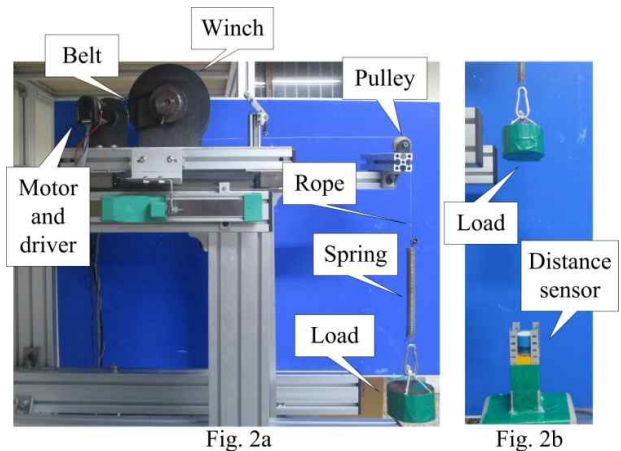


Fig. 2 Photos of experimental apparatus

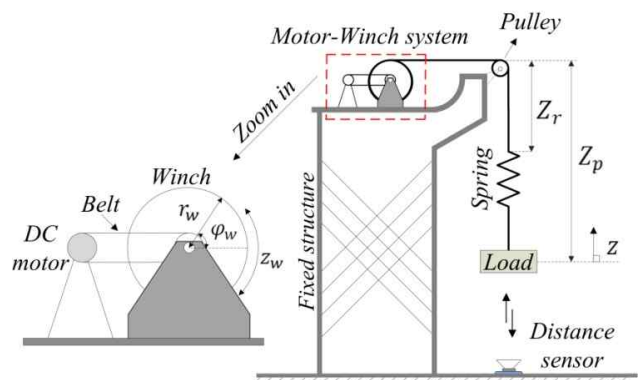


Fig. 3 Schematics of scaled crane model

The vertical rope dynamics due to the load moving can be calculated and approximated by the spring-mass-damper system. Exactly describing, it is estimated from the unwinded rope length  $Z_r$  and the load variation  $Z_p$  measured by distance sensor.

### 2.2 Estimation of motor-winch dynamics based on experimental data

In this paper, the motor-winch system dynamics is estimated by the Matlab Identification Toolbox and described as a linear transfer function. For this, at the first step, a chirp signal with frequency variations (from 0.01 Hz to 3 Hz in 60 seconds with 3 volts) is used to excite motor-winch system. Then the output is the rope length unwinded from winch as shown in Fig. 4 and Fig. 5. As the second step, we check the accuracy level of models by tuning the parameters and orders to obtain a representative model. For examples, the authors predefine the numbers of poles and zeros. With specifying poles and zeros, the fitting ratio between real system and models can be automatically calculated by using Matlab Tool as shown in Fig. 6 and Table 2.

Table 2 Fitting ratio of various motor-winch models for real plant

Model	Fitting ratio (%)
1 pole	76.28
2 poles	97.43
3 poles	94.34

Based on the comparison results, the authors choose the second order transfer function as the motor-winch model. As shown in Fig. 6 and Table 2, the second model is best one such that the identified model is obtained as follows:

$$\frac{z_w}{u} = \frac{1150}{s^2 + 9.524s + 0.01221} \quad (1)$$

Where  $z_w$  denotes the rope length, and  $u$  denotes the control input.

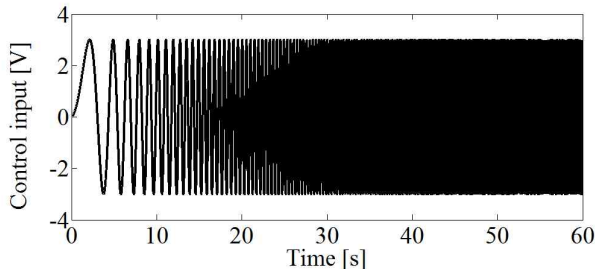


Fig. 4 Input signal to the motor-winch system

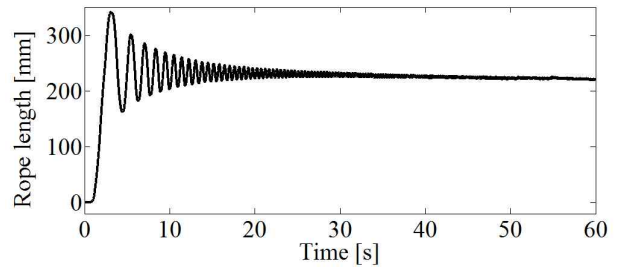


Fig. 5 Output signal(rope length variation denoted by  $Z_r$  in Fig. 3) of motor-winch system for the input signal given in Fig. 4

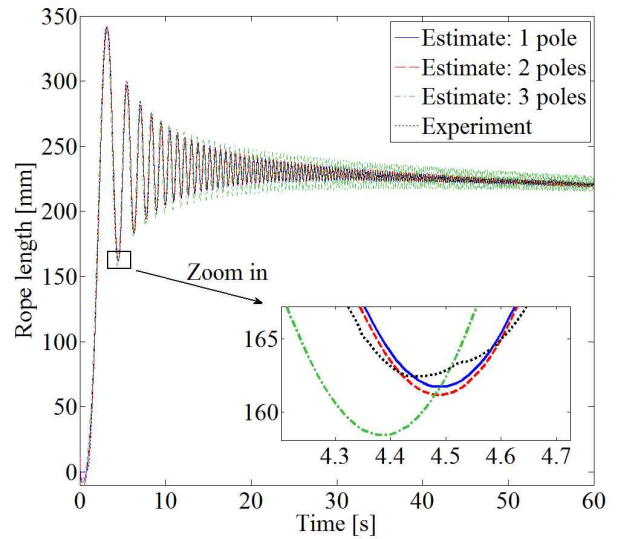


Fig. 6 Comparison results between simulation for linear models and experiment

### 2.3 Load motion dynamics

To identify load motion in vertical direction, the Newton/Euler method is introduced. Hence, it holds that:

$$m\ddot{Z}_p + d(\dot{Z}_p - \dot{Z}_r) + k(Z_p - Z_r) = 0 \quad (2)$$

with

$$Z_r = L_r(0) + z_w \quad (3)$$

According to Moon et al [11], while the crane moves the load in a vertical direction, the parameters of rope are time-varying and strongly depend on rope length. Then parameters for describing the rope dynamics are represented as following:

$$k = \frac{e_r c_r}{l_r}, \quad d = \frac{\beta c_r}{l_r}, \quad m_r = m_u l_r \quad (4)$$

where

- $k$  spring stiffness of rope
- $d$  damping constant of rope
- $m_r$  mass of rope

- $\beta$  constant of damping of rope  
 $e_r$  Young's modulus of rope  
 $c_r$  intersectional area of rope  
 $m_u$  mass per meter unit rope length

The overall normal rope length  $l_r$  is the distance between the winch and the load, and changed by winch operating which also affects the rope parameters as shown in Eq. (5).

$$l_r = L_r(0) + z_w \quad (5)$$

Where  $L_r(0)$  is the initial value of rope length.

And, it is assumed that the mass of rope is divided into two equal parts which are accumulated partly to the load and halfway to the winch. Then, an equivalent mass  $m$  in vertical motion is obtained as follows:

$$m = m_l + \frac{1}{2}m_r \quad (6)$$

Where  $m_l$  is the mass of load hung on to the end of rope.

From Eqs. (2)~(6), the second-order dynamic equation of load motion with  $Z_p$  can be expressed as follows:

$$\ddot{Z}_p = -\frac{\beta c_r}{l_r m} (\dot{Z}_p - \dot{Z}_r) - \frac{e_r c_r}{l_r m} (Z_p - Z_r) \quad (7)$$

### 3. Controller design

The authors introduce the control method based on an input/output linearization method for load position control as shown in Fig. 7.

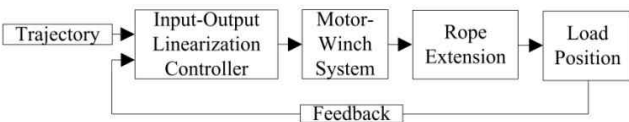


Fig. 7 Schematics of proposed control method

Based on Eqs. (1)~(7), the state space equation for load motion can be expressed. Before forming the state space equation of this nonlinear system, it is necessary to define state variables. Let us define the states as follows:

$$x = \begin{bmatrix} x_1 \\ x_2 \\ x_3 \\ x_4 \end{bmatrix} = \begin{bmatrix} z_w \\ \dot{z}_w \\ Z_p \\ \dot{Z}_p \end{bmatrix} \quad (8)$$

Where  $x_1$  is the rope length,  $x_2$  is the winding/unwinding rope velocity,  $x_3$  is the load position and  $x_4$  is the load moving velocity.

The state equation is created with previous kinetics

equations and the state definitions defined by Eq. (9).

$$\begin{cases} \dot{x} = f(x) + g(x)u \\ y = h(x), t \geq 0 \end{cases} \quad (9)$$

where

$$f(x) = \begin{bmatrix} x_2 \\ -0.01221x_1 - 9.524x_2 \\ x_4 \\ \frac{k}{m}x_1 + \frac{d}{m}x_2 - \frac{k}{m}x_3 - \frac{d}{m}x_4 + \frac{k}{m}L_r(0) \end{bmatrix} \quad (10)$$

$$g(x) = [0 \ 1150 \ 0 \ 0]^T \quad (11)$$

$$h(x) = [0 \ 0 \ 1 \ 0] \quad (12)$$

Following Eqs. (4)~(5) in Section 2.2, the spring stiffness  $k$ , damping constant  $d$  of the rope and equivalent mass  $m$  can be calculated by changing length of rope.

However, the parameters  $e_r$  and  $\beta$  of the rope used in experiment are hardly measured, and the length of the rope changes in the short operating range. Then, the authors assume that the damper constant  $d$  is neglected. And a spring (with stiffness coefficient  $k_r$ ) is inserted (between the end of rope and the load) to consider rope extension made by moving up and down the load. It is illustrated in Fig. 2 and Fig. 3.

With the assumptions and considering the inserted spring, then the equivalent mass  $m$  can be re-calculated as follows:

$$m \approx m_l \quad (13)$$

also, the Eq. (10) can be written as follows:

$$f(x) = \begin{bmatrix} x_2 \\ -0.01221x_1 - 9.524x_2 \\ x_4 \\ \frac{k_r}{m}x_1 - \frac{k_r}{m}x_3 + \frac{k_r}{m}L_r(0) \end{bmatrix} \quad (14)$$

In the input-output linearization theory, the SISO system is said to have output relative degree  $r_g$  in a region  $R^n$  if  $\forall x \in R^n$  as follows:

$$\begin{cases} L_g L_f^i h_{1(x)} = 0 \ \forall i = 0, 1, \dots, r_g - 2 \\ L_g L_f^{r_g - 1} h_{1(x)} \neq 0, \ \forall x \in R^n \end{cases} \quad (15)$$

Following the conditions in Eq. (15), the derivative  $\dot{y}$  is given by:

$$\dot{y} = \frac{\partial h}{\partial x} [f(x) + g(x)u] = L_f h(x) + L_g h(x)u \quad (16)$$

with

$$\frac{\partial h}{\partial x} f(x) = L_f h(x) \quad (17)$$

$$\frac{\partial h}{\partial x} g(x) = L_g h(x) \quad (18)$$

The Eqs. (17) and (18) are called as the Lie Derivative of

$h$  and  $g$  with respect to  $f$ , respectively.

In Eq. (18),  $L_g h_{(x)} u = 0$ . Then,  $\dot{y} = L_f h_{(x)}$  which is independent of  $u$ . Repeating, the second derivative  $\ddot{y}$  and third derivative  $y^{(3)}$  are also independent of  $u$ . The  $u$  appears in the equation of the fourth derivative  $y^{(4)}$  with a nonzero coefficient as shown in bellows:

$$\begin{aligned} y^{(4)} &= \frac{\partial(L_f h)}{\partial x} [L_f h_{(x)} + L_g h_{(x)} u] \\ &= L_f^4 h_{(x)} + L_g L_f^3 h_{(x)} u \end{aligned} \quad (19)$$

with

$$L_g L_f^0 h_{(x)} = L_g(x_3) = [0 \ 0 \ 1 \ 0] \begin{bmatrix} 0 \\ 1150 \\ 0 \\ 0 \end{bmatrix} = 0 \quad (20)$$

$$L_g L_f^1 h_{(x)} = L_g(x_4) = [0 \ 0 \ 0 \ 1] \begin{bmatrix} 0 \\ 1150 \\ 0 \\ 0 \end{bmatrix} = 0 \quad (21)$$

$$\begin{aligned} L_g L_f^2 h_{(x)} &= L_g \left( \frac{k_r}{m} x_1 - \frac{k_r}{m} x_3 + \frac{k_r}{m} L_r(0) \right) \\ &= \begin{bmatrix} \frac{k_r}{m} & 0 & -\frac{k_r}{m} & 0 \end{bmatrix} \begin{bmatrix} 0 \\ 1150 \\ 0 \\ 0 \end{bmatrix} = 0 \end{aligned} \quad (22)$$

$$\begin{aligned} L_g L_f^3 h_{(x)} &= L_g \left( \frac{k_r}{m} x_2 - \frac{k_r}{m} x_4 \right) \\ &= \begin{bmatrix} 0 & \frac{k_r}{m} & 0 & -\frac{k_r}{m} \end{bmatrix} \begin{bmatrix} 0 \\ 1150 \\ 0 \\ 0 \end{bmatrix} = 1150 \frac{k_r}{m} \neq 0 \end{aligned} \quad (23)$$

Clearly, following the model given in Eq. (9), the order of the system is 4, and the output relative degree is 4 ( $r_g = 4$ ).

It can be seen that from Eq. (24), the control law is derived via the input-output linearization method and written as follows:

$$u = \frac{\nu}{L_g L_f^3 h_{(x)}} \quad (24)$$

with trajectory tracking control law  $\nu$  given by:

$$\nu = y_{ref}^{(4)} - k_0 e_r - k_1 \dot{e}_r - k_2 \ddot{e}_r - k_3 e_r^{(3)} \quad (25)$$

$$e_r = y_{ref} - y \quad (26)$$

Where  $y_{ref}$  denotes the target trajectory input.  $k_0, k_1, k_2$  and  $k_3$  are state feedback gains. And the dynamics of the closed-loop tracking error  $e_r$  is given by:

$$e_r^{(4)} + k_0 e_r + k_1 \dot{e}_r + k_2 \ddot{e}_r + k_3 e_r^{(3)} = 0 \quad (27)$$

The dynamics of tracking error  $e_r$  can be represented by state-space form where the state vectors are defined as follows:

$$e = [e_r \ \dot{e}_r \ \ddot{e}_r \ e_r^{(3)}]^T \quad (28)$$

$$\dot{e} = \begin{bmatrix} 0 & 1 & 0 & 0 \\ 0 & 0 & 1 & 0 \\ 0 & 0 & 0 & 1 \\ 0 & 0 & 0 & 0 \end{bmatrix} e + \begin{bmatrix} 0 \\ 0 \\ 0 \\ 1 \end{bmatrix} q \quad (29)$$

$$q = -[k_0 \ k_1 \ k_2 \ k_3] e \quad (30)$$

As easily verified, system (29) is controllable. Then the state feedback gains ( $k_0, k_1, k_2$  and  $k_3$ ) can be designed by using any linear control design technique, such as the LQR design which minimizes the cost function.

$$J = \frac{1}{2} \int_0^\infty (e^T Q e + q^T R q) dt, \quad Q \geq 0, R > 0 \quad (31)$$

## 4. Experimental results

In this section, the experimental results with proposed controller are presented with comparison study.

The proposed control system is represented by Fig. 8.

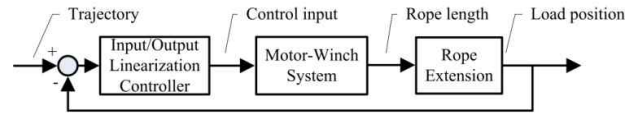


Fig. 8 Schematic diagram for experiment with proposed control approach

### 4.1 Load motion dynamics

In this paper, the stiffness coefficient  $k_r$  is identified by experiment result shown in Fig. 9~Fig. 11. As previously mentioned, a spring is inserted on purpose to consider rope extension which may be made by moving up and down the load in the real case.

At first, let's try to identify the spring dynamics with stiffness. For this, the test signal shown in Fig. 10 input to the motor-winch system. In the result, as the responses, the winching force, load position and rope length variation are illustrated in Fig. 11 and Fig. 12, respectively. It is clear that a rope model with load is represented as bellows:

$$m \ddot{Z}_p + k_r Z_p = f \quad (32)$$

Using the experiment results shown in Figs. 9~11 and Eq. (32), the spring stiffness coefficient  $k_r$  can be identified. Then, the stiffness coefficient  $k_r$  is obtained as bellows:

$$k_r = 250 \text{ [N/m]} \quad (33)$$

With the calculated stiffness  $k_r$  about the inserted spring, the load position and rope length variation can be calculated as shown in Fig. 12 where the same test signal given in Fig. 9 is used.

Then, let's check the comparison results. The simulation



and experiment results are shown in Fig. 13 which is uncontrolled cases.

It is clear that the obtained model for real plant is acceptable and useful for control system design.

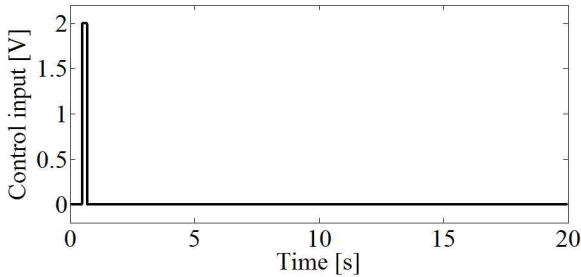


Fig. 9 The input signal used to excite the motor-winch system

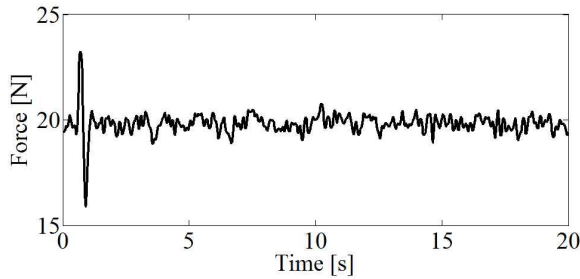


Fig. 10 Force produced from the motor-winch system

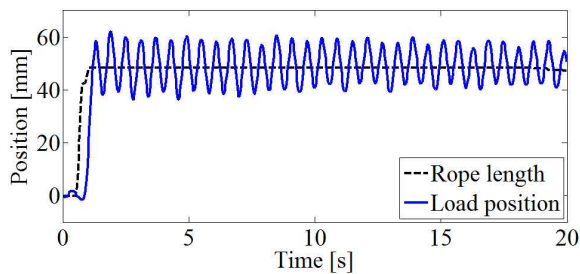


Fig. 11 Load position and rope length for impulse type control input given in Fig. 10 (experiment)

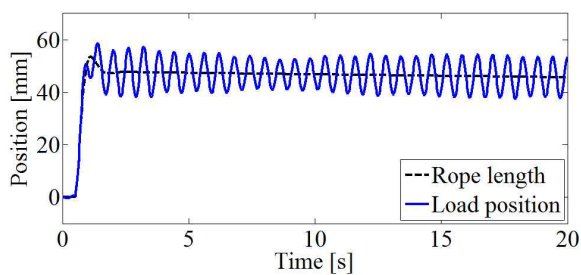


Fig. 12 Load position and rope length variation (simulation results using estimated parameter values, uncontrolled case)

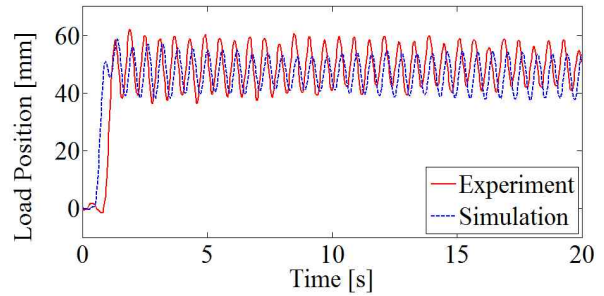


Fig. 13 Comparison results by simulation and experiment (uncontrolled case)

#### 4.2 Controller design for load motion control

Based on the previous result, the authors conduct experiment for controlling load position and suppressing vertical vibration of load in the scaled crane system.

In the experiment, the feedback gains given in Eq. (30) are calculated as  $k_0 = 2000$ ,  $k_1 = 1800$ ,  $k_2 = 1060$  and  $k_3 = 105$ .

And, the reference trajectories are given as two types for evaluating the designed control system. Exactly describing, the first case target trajectory is step type and another one is ramp type with defined slew rate.

More precise informations are described in Table 3.

Table 3 The input trajectory

Case	Load target position [mm]	Target trajectory slew rate [mm/s]
1	100	0
2	100	50

Let us evaluate the experiment results of the first case (without slew rate).

Fig. 14 shows the load position control performances when the reference target is given by step type. Where, (a) is the control input, and (b) shows the rope length released from the winch. Finally, (c) illustrates the controlled (solid line) and uncontrolled load position (dashed line). However, for the step type target trajectory, the proposed control system makes good control performance without any residual vibration in the steady state.

But, in the uncontrolled case, the residual vibration is continuously shown and needed to be suppressed.

In the second try (with slew rate 50 [mm/s]), let us check time response with ramp type reference target trajectory. In fact, it is general that the reference signal is given by ramp type with proper slew rate for real system. With considering of real operating condition, the authors obtained

experiment results which are illustrated in Fig. 15.

As we can see, there is no notable difference comparing with previous results in the steady state. But, we can find out more improved transient response in the proposed control scheme as expected.

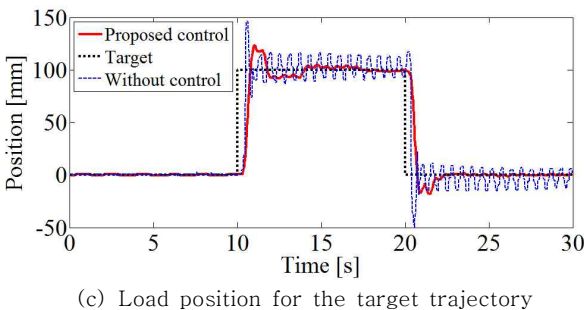
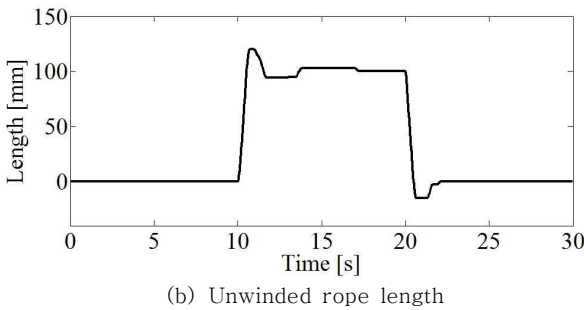
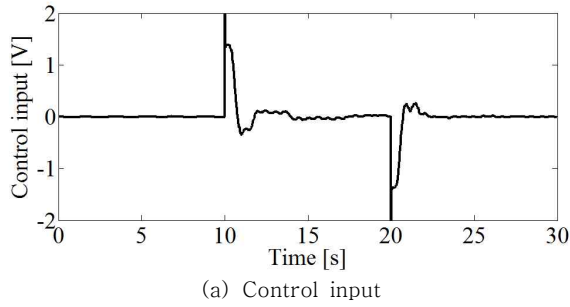


Fig. 14 Experiment results when the target trajectory is step type

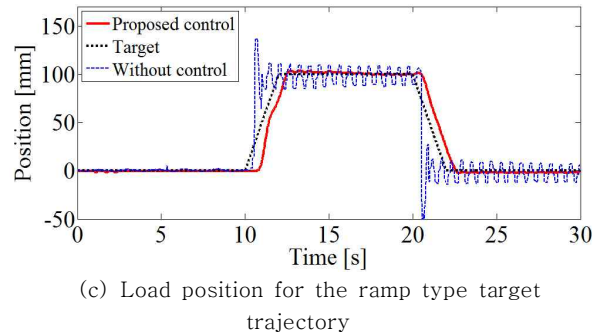
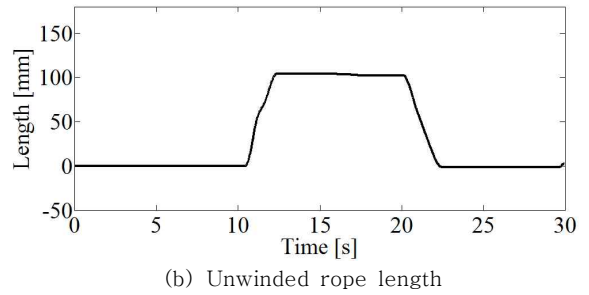
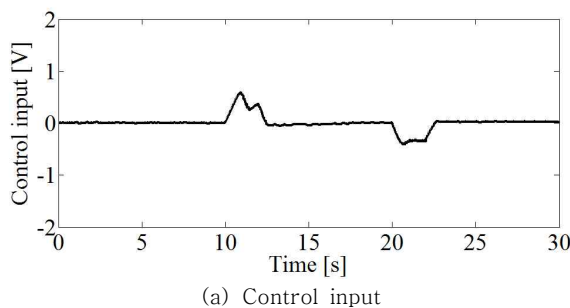


Fig. 15 Experiment results when the target trajectory is ramp type

## 5. Conclusions

In this paper, the authors investigated a control strategy for controlling load position and suppressing vertical vibration in offshore crane system under external factors such as rope extension etc.

Especially, it is considered how we can move a load and place it on the specified place using offshore crane system which are installed on the marine vessel.

Furthermore, there exists strong spring coefficient due to rope extension which is a key factor of undesirable load vibration. Therefore, the accurate winch system control and vibration suppressing of hanged load is necessary.

To obtain a solution for this issue, the authors designed a control system using input-output linearization method. The experimental results indicated that the proposed strategy works well and can be implemented to the real system.

## Acknowledgment

This work was supported by the National Research Foundation of Korea (NRF) grant funded by the Korea Government (Ministry of Education) (No. NRF-2015R1D1A1A09056885)

## References

- [1] Abdel-Rahman E. M., Nayfeh A. H. and Masoud Z. N.(2003), "Dynamics and control of cranes: a review", *Journal of Vibration and Control*, Vol. 9, No. 7, pp. 863-908.
- [2] Almutairi N. B. and Zribi M.(2009), "Sliding mode control of a three-dimensional overhead crane", *Journal of Vibration and Control*, Vol. 15, No. 11, pp. 1679-1730.
- [3] Fang Y. C., Wang P. C. and Sun N.(2014), "Dynamics analysis and nonlinear control of an offshore boom crane", *IEEE Transactions On Industrial Electronics*, Vol. 61, No. 1, pp. 414-427.
- [4] Hatleskog J. T. and Dunnigan M. W.(2007), "Passive compensator load variation for deep-water drilling", *IEEE Journal of Oceanic Engineering*, Vol. 32, No. 3, pp. 593-602.
- [5] Hatleskog J. T. and Dunnigan M. W.(2012), "An impedance approach to reduce the contact-instability whilst drilling with active heave compensation", *Ocean Engineering*, Vol. 49, pp. 25-32.
- [6] Jolevski D. and Bego O.(2015), "Model predictive control of gantry/bridge crane with anti-sway algorithm", *Journal of Mechanical Science Technology*, Vol. 20, No. 7, pp. 827-834.
- [7] Kalmari J., Backman J. and Visala A.(2014), "Nonlinear model predictive control of hydraulic forestry crane with automatic sway damping", *Computer and Electronics in Agriculture*, Vol. 109, No. 1, pp. 36-45.
- [8] Korde U. A.(1998), "Active heave compensation on drill-ships in irregular waves", *Ocean Engineering*, Vol. 25, No. 7, pp. 541-561.
- [9] Kotera T.(1978), "Vibrations of string with time-varying length", *Transactions of the Japan Society of Mechanical Engineers*, Vol. 60, pp. 765-768.
- [10] Messineo S. and Serrani A.(2009), "Offshore crane control based on adaptive external models", *Journal of the International Federation of Automatic Control*, Vol. 45, No. 110, pp. 2546-2556.
- [11] Moon S. M., Huh J., Hong D., Lee S. and Han C. S.(2015), "Vertical motion control of building facade maintenance robot with built-in guide rail", *Robotics and Computer-Integrated Manufacturing*, Vol. 31, No. 1, pp. 11-20.
- [12] Nam B. W., Hong S. Y. and Kim Y. S.(2013), "Effects of passive and active compensators on deepwater lifting operation", *International Journal of Offshore and Polar Engineering*, Vol. 23, No. 1, pp. 33-37.
- [13] Ngo Q. H. and Hong K. S.(2010), "Sliding-mode anti-sway control of an offshore container crane", *IEEE/ASME Transactions on Mechatronics*, Vol. 17, No. 2, pp. 201-209.
- [14] Ouyang H., Zhang G., Deng X. and Wang D.(2016), "Load vibration reduction in rotary cranes using robust two-degree-of-freedom control approach", *Advances in Mechanical Engineering*, Vol. 8, No. 3, pp. 1-11.
- [15] Sagatun S. I.(2002), "Active control of underwater installation", *IEEE Transactions on Control System Technology*, Vol. 10, No. 5, pp. 743-748.
- [16] Sun N., Fang Y. F. and Chen H. A.(2015), "A new anti-swing control method for underactuated cranes with unmodeled uncertainties: theoretical design and hardware experiments", *IEEE Transactions on Industrial Electronics*, Vol. 62, No. 1, pp. 453-465.
- [17] Tuan L. A. and Lee S. G.(2013), "Sliding mode of double-pendulum crane system", *Journal of Mechanical Science and Technology*, Vol. 27, No. 6, pp. 1863-1873.
- [18] Viet L. A. and Park Y. A.(2015), "A cable-passive damper system for sway and skew motion control of a crane spreader", *Shock and Vibration*, Vol. 25, No. 1, pp. 1-11.
- [19] Wu Z., Xia X. H. and Zhu B.(2015), "Model predictive control for improving operational efficiency of overhead cranes", *Nonlinear Dynamics*, Vol. 79, No. 4, pp. 2639-2657.

---

Received 9 June 2017

Revised 20 October 2017

Accepted 23 October 2017